

INTERACTION OF LASER RADIATION WITH MATTER

PACS numbers: 71.20.Mq; 72.80.Cw; 42.65.Re
DOI: 10.1070/QE2012v042n10ABEH014872

Excitation of the electronic subsystem of silicon by femtosecond laser irradiation

V.V. Kononenko, E.V. Zavedeev, M.I. Latushko, V.P. Pashinin, V.I. Konov, E.M. Dianov

Abstract. **We have studied processes initiated in the bulk of single-crystal silicon by local excitation of its electronic subsystem with femtosecond IR laser pulses (λ = 1.2 μm, τ_{FWHM} = 250 fs). IR femtosecond interferometry has been used for the first time to measure the refractive index of the irradiated zone. Using the interference images obtained in our experiments, we have reconstructed the dynamics of the electron–hole plasma generated near the axis of a focused laser beam. Experimental data have been compared to relevant numerical simulation results obtained in a simple, two-photon absorption model.**

Keywords: *femtosecond laser radiation, fast processes in solids, femtosecond interferometry.*

1. Introduction

Research interest in processes induced in transparent solids by high-intensity light is due to two main causes. A standard cause is that, when crystals and glasses are used in laser engineering, a detailed understanding is required of photoinduced processes in the medium and how these are related to the characteristics of the light. This is of particular importance for light generation and amplification, as well as in the case of frequency conversion, because photoinduced processes in a medium typically have a very strong effect on both the efficiency of nonlinear conversion and the stable state of a gain element, in particular on its optical damage resistance. The other cause is the relatively recent revival of interest in the possibility of radiation-induced local structural changes [1]. In current practice, UV radiation from excimer lasers is used to modify various glasses [2, 3]. Relatively recent studies have demonstrated the possibility of obtaining similar results using high-intensity ultrashort pulses, where a key role is played by nonlinear absorption [4, 5]. This approach has the advantage that, away from the laser beam waist, the material is transparent, which allows one, in principle, to structure thick samples.

The experiments described in this paper, aimed at exciting the electronic subsystem of crystalline silicon by femtosecond laser radiation, were prompted by recent reports that not only the structure of the lattice of glass but also that of crystals can be transformed [6–8]. The thermodynamics of such structures has been studied little, but it seems likely that an amorphous phase in a microvolume is in quasi-equilibrium with the rest of the lattice and is similar to the amorphous phase that results from the low-temperature growth of thin films. The ability to produce such structures through laser processing is a new issue of great fundamental interest.

The choice of silicon as the material to be studied is dictated by the following considerations: First, it is well known that thin silicon films may be amorphous. Second, silicon is used in modern electronics so widely that a search for technologies capable of producing photonic structures (waveguides, couplers, gratings and others) in crystals is of considerable practical interest [9, 10]. Finally, even though the influence of laser radiation on the surface of silicon and the associated excitation and relaxation processes in its electronic subsystem have been the subject of rather extensive studies [11–13], there is currently very little data on nonlinear effects in the bulk of c-Si. To our knowledge, sufficiently specific laser processing of a quartz/silicon bilayer structure has been demonstrated in only one study, that by Nejadmalayeri et al. [14]. They produced a buried waveguide under a quartz film, but the question of whether laser patterning is possible deep in the bulk of silicon still remains open.

2. Experimental

The laser system used included a Ti:sapphire oscillator (Tsunami, Spectra Physics) and a regenerative amplifier (Spitfire, Spectra Physics) operating at 800 nm (Fig. 1). To ensure penetration of the beam into the bulk of the sample, we employed a Spectra Physics OPA-800 parametric amplifier, which allowed us to obtain femtosecond pulses at wavelengths from 1.1 to 3.0 μm, with pulse energies up to 100 μJ and a repetition rate of 1 kHz. The pulse energy was varied using attenuation filters. The laser beam was focused by an f = 8 mm aspherical lens into a silicon sample (30×10×3 mm) polished on four faces. Since a wide range of irradiation energies, up to the highest possible one in the described system, was used in our experiments, the distance from the laser caustic to the front face of the sample was sufficiently large, about 4 mm. This depth was chosen in order to prevent laser damage of the sample surface at the highest irradiation energy.

To visualise the irradiation results, we used the pump–probe technique (Fig. 1). In a standard approach (see e.g. Ref. [12]), one measures the reflectivity of the sample surface for a probe beam during and after exposure of the sample to a laser pulse. In the experiments under consideration, the beam was divided into two parts by a beam splitter, and the

V.V. Kononenko, E.V. Zavedeev, M.I. Latushko, V.P. Pashinin, V.I. Konov A.M. Prokhorov General Physics Institute, Russian Academy of Sciences, ul. Vavilova 38, 119991 Moscow, Russia; e-mail: vitali.kononenko@nsc.gpi.ru;
E.M. Dianov Fiber Optics Research Center, Russian Academy of Sciences, ul. Vavilova 38, 119333 Moscow, Russia

Received 23 March 2012; revision received 23 July 2012
Kvantovaya Elektronika **42** (10) 925–930 (2012)
Translated by O.M. Tsarev

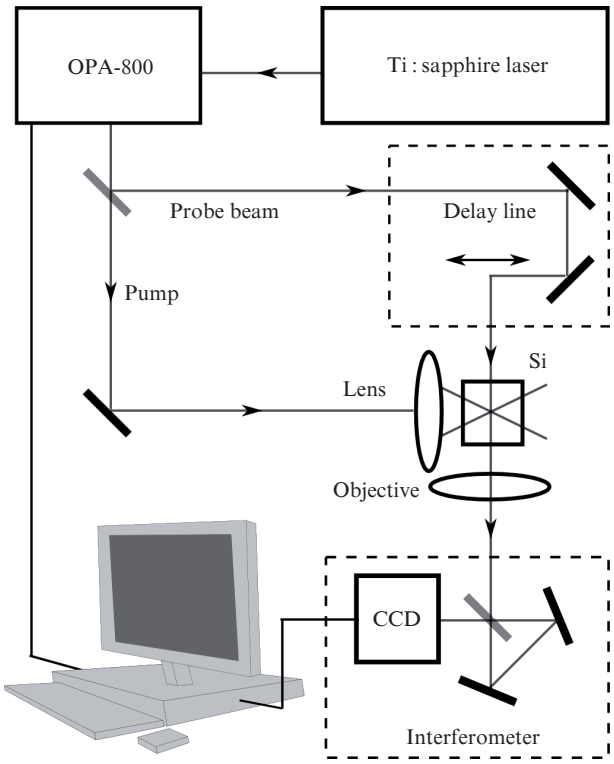

Figure 1. Schematic of the experimental setup.

probe beam passed through a delay line and then impinged on the lateral surface of the sample. The image of the region exposed to the high-intensity laser light was projected onto the plane of the visualiser at a magnification of 30×. As a visualiser, we used an image converter whose spectral sensitivity range extended up to 1.3 μm. The image produced on the luminescent screen of the image converter was projected onto a CCD array detector, digitised and processed to give real-time information about the state of the irradiated zone. Since the fundamental absorption edge of silicon lies at 1.1 μm, the wavelength used in our experiments was 1.2 μm (Fig. 2). This allowed us, on the one hand, to achieve a sufficiently high sensitivity of the detector and, on the other, to ensure that the crystal was transparent to the pump and probe beams.

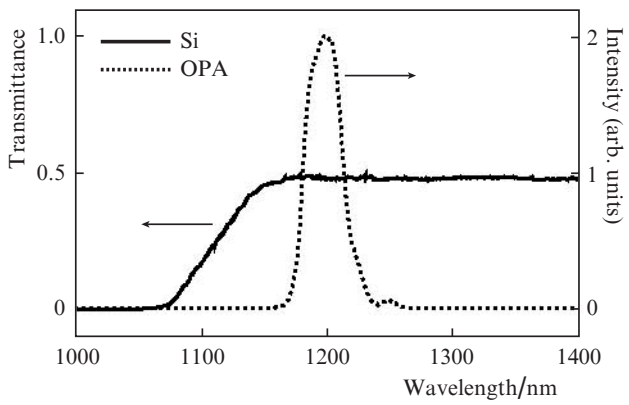

Figure 2. Emission spectrum of the OPA-800 parametric amplifier and transmission window of silicon.

A key method for gaining quantitative information about the state of the material during and after laser irradiation was femtosecond interferometry [15, 16]. A Sagnac interferometer was placed between a projection objective lens and the image converter. The mirrors of the interferometer were adjusted so that the angle between the beams was almost zero, producing a broadband interference pattern on the array detector. The beam splitter in the interferometer had the form of a wedge with an angle of ~3°, so that the images produced in the two arms of the interferometer did not overlap on the array detector. Thus, the interference pattern observed on a display was produced by two beams, both having a local phase disturbance due to the change in the index of refraction, n, in the irradiated region. Since the interference fringes were rather broad, their shift in the irradiated region led to local changes in image brightness, which allowed us to evaluate the change in n.

In our experiments, two interference images were obtained for particular irradiation conditions: with an excitation pulse (information image) and with no excitation (background image). The difference image obtained on a computer contained only information about the change in n. This approach enabled a substantial improvement in online measurement accuracy, which was determined under these conditions primarily by the interferometer mirror jitter between consecutive information and background images. Minimising mechanical vibrations and taking a number of images under identical irradiation conditions, with subsequent averaging, allowed us to determine the phase of the electromagnetic (EM) wave in the probe beam with a sensitivity $\delta\phi$ better than 10^{-2}. The 'thickness' of the probed region was roughly equal to the laser beam diameter, $d \approx 10$ μm. Therefore, the smallest change in the refractive index of the medium that could be detected with our experimental setup at a femtosecond time resolution was $\delta n = \delta\phi\lambda/d \approx 10^{-3}$.

3. Results and discussion

Figure 3 illustrates the propagation of a femtosecond laser pulse through a silicon crystal. For convenience, only one image of the irradiated zone is left in the photographs. An increase in local brightness (a bright spot) in the picture corresponds to an increase in the refractive index. And vice versa, a reduction in brightness (long dark band) means a decrease in n. It is well seen in the series of photographs that the refractive index of the crystal is a strong function of time. The influence of the EM field on the medium first causes n to increase, which is due to the polarisability nonlinearity in the medium – the so-called Kerr effect. One can clearly see a light cloud propagating through the crystal at the speed of light, with a brightness proportional to the light intensity at a given point of the sample. The cloud is in fact an 'image' of the wave packet, and by analysing it one can in particular evaluate spatial and temporal parameters of the pulse. In our experiments, the pulse duration was $\tau_{FWHM} = 250$ fs and the 1/e radius of the Gaussian beam in its caustic was $r_0 = 15$ μm.

Note that, in this approach to intensity evaluation, there is no need to take into account any transformations of the beam wavefront or any pulse energy losses: reflection from the sample surface, aberrations, linear or nonlinear scattering or absorption losses when light propagates through the crystal or any others. The light intensity was estimated as $I = \Delta n/n_2$. The constant parameter n_2 was estimated for the lowest energy in our experiments, with nonlinear effects

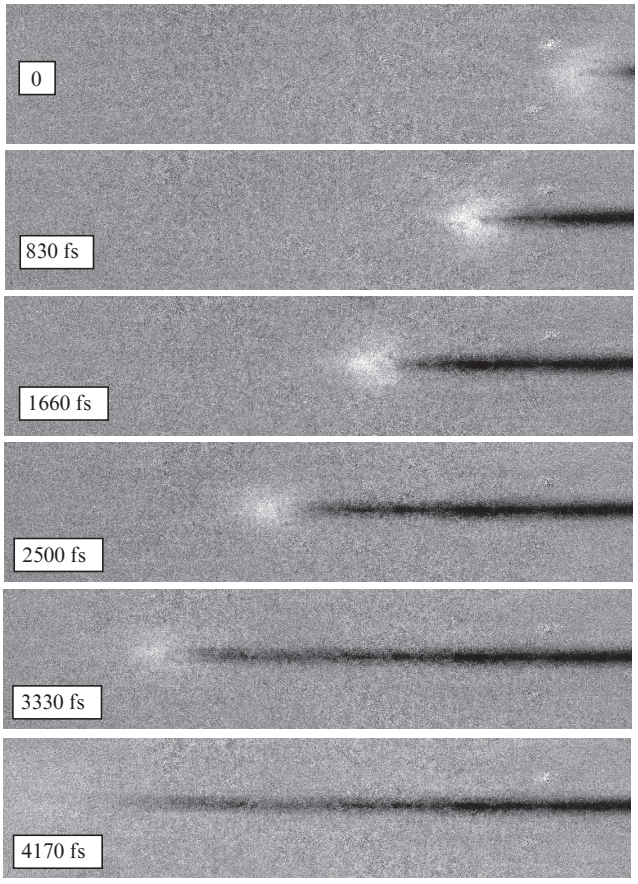

Figure 3. Interference images obtained during the propagation of a femtosecond IR pulse through a silicon crystal. The time delays are indicated in each panel. The horizontal size of the images is 400 μm. Their contrast is increased to improve visualisation.

neglected. We obtained $n_2 = 8 \times 10^{-14}$ cm^2 W^{-1}, in reasonable agreement with the 2.6×10^{-14} cm^2 W^{-1} reported by Dinu et al. [17].

Further exposure to the field leads to the ionisation of the covalent bonds in the crystal, thus promoting electrons to the conduction band and producing holes in the valence band. As a result, the refractive index of the medium drops sharply. The plasma lifetime was measured to be ~10 ns, in good agreement with the characteristic carrier lifetimes in the bulk of crystalline silicon in the intrinsic regime.

The plasma generation time is very short, of the same order as the pulse duration, so a plasma cloud forms in a region still 'occupied' by the wave packet, producing a complex interference pattern in the region where the change in n switches from positive to negative.

If the carrier concentration is low and the corresponding change in n can be neglected, the nonlinear polarisation of the medium is only determined by the Kerr effect. In this case, an interference photograph is in fact an autocorrelation trace of the laser pulse and, as mentioned above, the actual excitation dynamics in the medium are easy to reconstruct. If the contribution of the electron–hole plasma is significant, the autocorrelation integral contains a nonlinear factor determined by the light absorption mechanism.

To solve the inverse problem and reconstruct the dynamics of Δn, one should first make relevant assumptions regarding the absorption mechanism. Nevertheless, the advantage of this approach is that interference measurements can be made with as small a time step as desired. The smallest change in time delay is in fact only limited by the positioning accuracy of the elements of the optical system. The dynamics of the state of the material in the irradiated zone can then be reconstructed with a time resolution considerably better than the pulse duration. Comparing the dynamics of the interference signal evaluated using *a priori* theoretical equations to that inferred from experimental data, one can, in principle, assess the relevance of models for the laser excitation of the electronic subsystem of solids.

In the case of silicon, which has a band gap of 1.12 eV, two photons ($\hbar\omega$ = 1.03 eV) are needed to promote an electron to the conduction band. At the light intensity that can be reached under the conditions of this study, $I \sim 10^{11}$ W cm^{-2}, the two-photon absorption in the medium can be estimated as $\alpha_{\rm tpa} = \beta I \approx 50$ cm^{-1}, where $\beta = 0.53 \times 10^{-9}$ cm W^{-1} is the two-photon absorption coefficient of silicon at $\lambda = 1.2$ μm [18]. At the same time, the transmission spectrum in Fig. 2 demonstrates that the absorption in our sample at this wavelength certainly does not exceed 1%, suggesting that the single-photon absorption coefficient $\alpha_{\rm spa}$ does not exceed 0.03 cm^{-1}. Therefore, under the conditions of this study, two-photon absorption should be expected to prevail in the femtosecond excitation of the electronic subsystem of silicon.

The intensity of a pump pulse propagating along the z axis in a Cartesian coordinate system (Fig. 4) can be written in the form

$$I^{\rm e}(x,y,z,t) = I_0^{\rm e}\frac{r_0^2}{r^2(z)}\exp\left(-\frac{x^2+y^2}{r^2(z)}\right)\exp\left[-\frac{(z-vt)^2}{(v\tau)^2}\right],$$

where $r(z) = \sqrt{r_0^2 + (\lambda^2 z^2)/(4\pi^2 r_0^2)}$; r_0 is the radius of the Gaussian beam in the centre of its waist; $\tau = \tau_{\rm FWHM}/2\sqrt{\ln 2}$ is a parameter characterising the pulse duration; and v is the speed of light in the medium.

The net contribution of the Kerr effect and the polarisation induced by free carriers – which can be taken into account using the Drude model – to the refractive index change can be written as

$$\Delta n(x,y,z,t) = n_2 I^{\rm e} - \frac{2\pi e^2}{n_0\omega^2}\frac{N}{m^*}, \qquad (1)$$

where $n_2 = 2.6 \times 10^{-14}$ cm^2 W^{-1} is the Kerr coefficient [17]; $n_0 = 3.5$ is the refractive index of silicon; $\omega = 1.57 \times 10^{15}$ Hz is the laser frequency; e is the electron charge; $m^* = (m_{\rm e}^{-1} + m_{\rm h}^{-1})^{-1}$ is the effective optical mass of the carriers; and N is their concentration. In the case of two-photon absorption, we have

$$N(x,y,z,t) = \frac{\beta(I^{\rm e})^2\tau_{\rm FWHM}}{2\hbar\omega}, \qquad (2)$$

where $\hbar\omega$ is the photon energy and $\beta = 0.53 \times 10^{-9}$ cm W^{-1} is the two-photon absorption coefficient of silicon at $\lambda = 1.2$ μm [18].

The intensity of the probe beam, whose propagation along the y axis has a time delay $t_{\rm d}$ relative to the pump pulse, can be written as

$$I^{\rm p}(t') = I_0^{\rm p}\exp\left[-\frac{(t'+t_{\rm d})^2}{\tau^2}\right].$$

Consider a thin layer, $v\mathrm{d}t'$, of the probe pulse (Fig. 4), in which the energy density is

$$\mathrm{d}F^{\mathrm{p}}(t') = I_0^{\mathrm{p}} \exp\left[-\frac{(t'+t_{\mathrm{d}})^2}{\tau^2}\right]\mathrm{d}t'.$$

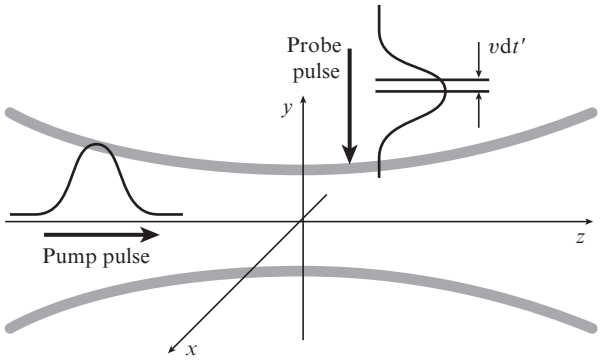

Figure 4. Configuration used in the numerical simulation of the formation of an interference image.

Its position in space varies over time: $y(t) = v(t + t' + t_{\mathrm{d}})$. The nonlinear polarisation wave Δn (1) induced by the pump pulse propagates in space and introduces a phase delay into the initially planar front of the probe beam:

$$\Delta\phi(x,z,t') = \int_{-\infty}^{\infty} \frac{1}{\lambda}\Delta n(x,y(t),z,t)\mathrm{d}(y(t)).$$

Thus, the change in the brightness of the interference pattern at point (x, z) relative to its undisturbed state can be accurately calculated as a function of t_{d}:

$$B(x,z,t_{\mathrm{d}}) = \int_{-\infty}^{\infty} \sin(\Delta\phi(x,z,t'))\mathrm{d}F^{\mathrm{p}}(t')$$

$$= I_0^{\mathrm{p}} \int_{-\infty}^{\infty} \sin(\Delta\phi(x,z,t'))\exp\left[-\frac{(t'+t_{\mathrm{d}})^2}{\tau^2}\right]\mathrm{d}t'. \qquad (3)$$

It should be emphasised that, physically, it makes no sense to calculate the average phase shift of the probe beam because the characteristic 'thickness' of the excited zone varies rapidly. As mentioned above, if the absorption mechanism is known, one can, in principle, solve the inverse problem and assess the dynamics of $\Delta n(t)$ at a given point in space, but the approach used in this study is to directly compare calculation results and experimental data on the brightness of the interference pattern as a function of the time delay between pump and probe pulses.

Figure 5 illustrates the breakdown dynamics: the time variation of the relative brightness B of the interference pattern at the central point of the laser caustic of the pump pulse. Note that we observe the same behaviour throughout the range of pulse energies examined (0.03–90 μJ), and the variation in B is on the whole consistent with the clear physical picture described above. After approximately 500 fs, when the wave packet reaches the measurement point, the refractive index and image brightness begin to increase (nonlinear susceptibility); subsequently, they decrease (electron–hole plasma).

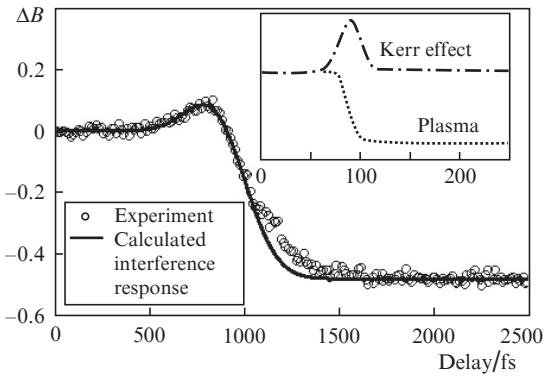

Figure 5. Temporal dynamics of the relative brightness of the interference pattern in the centre of the excitation beam caustic (laser pulse energy, 4.5 μJ).

Also presented in Fig. 5 are numerical simulation results obtained for the silicon photoexcitation process using (3). The simulation results are seen to agree well with the experimental data. There is some discrepancy at the end of the pulse: the generation rate seems to be lower than the theoretically predicted value. This feature in the temporal dynamics of n was observed at all the energies examined.

This can probably be interpreted as follows: The polarisability of a medium under laser excitation is known to depend on at least three parameters of the generated plasma. One of them is the concentration of free carriers, N, which, located in the conduction band, change the nature of the response of the medium to an EM field. Another parameter is the equilibrium density of occupied states, which influences the probability of interband transitions and, hence, the polarisability of the medium. At the observed electron–hole pair concentrations, this effect is rather weak, so it was left out of account in our estimates. Finally, the third parameter is the plasma temperature, which has a significant effect on the optical oscillator mass and, hence, on n [see Eqn (1)]. This dependence is rather strong: according to Sabbah and Riffe [12], $m^*_{300} = 0.156m_{\mathrm{e}}$ at room temperature in silicon and $m^*_{1985} = 0.205m_{\mathrm{e}}$ at $T =$ 1985 K. Assuming that a 'free' electron gains energy through inverse-bremsstrahlung absorption more rapidly than it transfers energy to the lattice, we conclude that plasma heating will favour a transient increase in polarisability. Note however that, under the irradiation conditions used in this study, carrier heating seems to be insufficient for significant impact ionisation of silicon.

Thus, the present experimental data can be described rather well in terms of a simple, two-photon absorption model which, in particular, neglects the effect of the nonlinear polarisation of the medium on the propagation of a wave packet. This does not at all mean that, at the laser pulse energies used in this study, self-focusing, plasma defocusing or other effects play an insignificant role. In contrast, recent work [19] has shown that, because of nonlinear effects, energy delocalisation in silicon reduces the energy density by more than a factor of 100 relative to the linear propagation of light. However, in our simulations, the dynamics of the variation in n were assessed at one point of the caustic on the optical axis, where the local intensity was monitored in fact from the degree of Kerr polarisation. This local approach allows the spatiotem-

poral modulation of the pump pulse to be left out of consideration.

The degree of such modulation and that of the associated wave packet delocalisation can be estimated from the data in Fig. 6, which shows the interference image brightness as a function of pulse energy for the irradiated zone. Curve (*1*) was obtained at the instant when the pulse passed through the point in question, and curve (*2*) was obtained 1 ps later. In fact, curve (*1*) describes the Kerr effect and curve (*2*) corresponds to the concentration of photogenerated carriers in the lattice. The two curves correlate well with one another, are substantially nonlinear and show well-defined logarithmic behaviour, with progressive saturation as the pulse energy increases. Moreover, at pulse energies above 20 μJ the concentration of photogenerated electrons and holes does not increase.

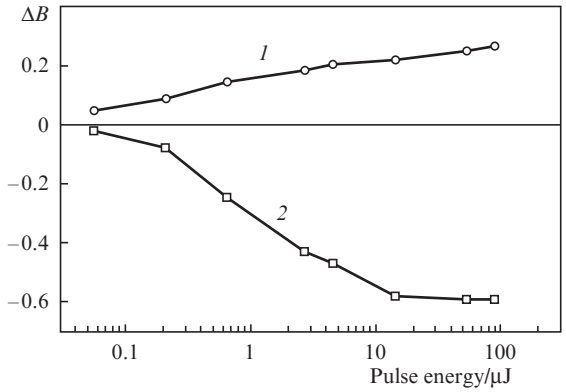

Figure 6. Effect of pump pulse energy on the changes in the relative brightness of interference patterns in response to (*1*) the Kerr polarisation of the medium and (*2*) the formation of an electron–hole plasma in silicon.

From these data, we derived the carrier concentration after a laser pulse as a function of laser fluence in the centre of the caustic (Fig. 7). The plasma density was evaluated using the Drude formula, and its highest value was 1.5×10^{20} cm^{-3}. It follows from the data in Fig. 7 that the absorption probability is, to a good approximation, proportional to the square of the light intensity up to laser fluences $F \approx 45$ mJ cm^{-2}. The two-photon absorption coefficient of silicon estimated from these data, $\beta = 0.46\times10^{-9}$ cm W^{-1}, approaches the 0.53×10^{-9} cm W^{-1} reported by Lin et al. [18] for $\lambda = 1.2$ μm.

Note the well-defined saturation of the carrier concentration for $F \geqslant 45$ mJ cm^{-2}. Such deviations from power-law behaviour for multiphoton absorption were observed earlier in semiconductors (see e.g. Refs [20, 21]) and, what is more, at the same plasma density, $N \approx 10^{20}$ cm^{-3}. This effect is commonly attributed to plasma defocusing, which leads to a sharp drop in light intensity at the point of breakdown. In our case, the scattering loss is taken into account, because the optical energy density is measured locally, from the nonlinear susceptibility of the medium. Note however that, in analysing interference images, we assume *a priori* that the temporal profile of the femtosecond pulse remains nearly Gaussian. If this condition is not satisfied at high plasma densities because of the wave packet delocalisation, the calculated local light intensity will be incorrect, which may be responsible for the inflection in the experimental curve (Fig. 7). An alternative explanation

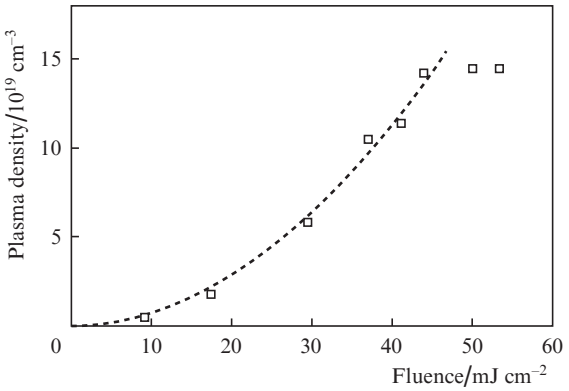

Figure 7. Electron–hole plasma density in silicon as a function of laser fluence.

is that this effect reflects the inherent nature of the excitation of the electronic subsystem of the medium; that is, for $N \geqslant 10^{20}$ cm^{-3}, photoinduced electronic transitions in silicon are suppressed.

4. Conclusions

We have studied processes induced in the bulk of single-crystal silicon by femtosecond IR laser pulses. The state of the material in the irradiated zone was monitored for the first time using IR femtosecond interferometry, which allowed us to estimate the Kerr coefficient n_2 of silicon: 8×10^{-14} cm^2 W^{-1}. In addition, we have proposed a simulation procedure that enables the formation of an interference image of the irradiated zone to be modelled based on *a priori* assumptions as to the carrier generation and recombination mechanisms. The advantage of this approach is that dynamic changes in a medium can be measured with a time resolution considerably better than the pulse duration, which allows one, in principle, to considerably improve the reliability of the theoretical models used.

We have assessed the dynamics of electron–hole plasma excitation in the bulk of silicon and the rate of plasma relaxation after the pulse. A simple model that takes into account only two-photon absorption in silicon is shown to adequately describe the observed dynamics of the polarisability of the medium in the bulk of the material in the case of strong nonlinearity. Moreover, the excited carrier concentration in silicon as evaluated in the Drude model is shown to be a quadratic function of laser fluence, which also suggests that the contribution of two-photon absorption prevails. From the data obtained, the two-photon absorption coefficient has been estimated at $\beta = 0.46\times10^{-9}$ cm W^{-1}.

Acknowledgements. This work was supported by the Russian Foundation for Basic Research (Grant No. 11-02-12242) and the Russian Academy of Sciences (basic research programme No. PRAN 13).

References

1. Primak W., Kampwirth R. *Appl. Phys.*, **39**, 5651 (1968).
2. Rothschild M., Ehrlich D.J., Shaver D.C. *Appl. Phys. Lett.*, **55**, 1276 (1989).
3. Allan D.C., Smith C., Borrelli N.F., Seward III T.P. *Opt. Lett.*, **21**, 1960 (1996).

4. Davis K.M., Miura K., Sugimoto N., Hirao K. *Opt. Lett*., **21**, 1729 (1996).
5. Glezer E.N., Milosavljevic M., Huang L., Finlay R.J., Her T.H., Callan J.P., Mazur E. *Opt. Lett*., **21**, 2023 (1996).
6. Gorelik T., Will M., Nolte S., Tuennermann A., Glatzel U. *Appl. Phys. A: Mater. Sci. Process.*, **76**, 309 (2003).
7. Apostolopoulos V., Laversenne L., Colomb T., Depeursinge C., Salathe R.P., Pollnau M., Osellame R., Cerullo G., Laporta P. *Appl. Phys. Lett.*, **85**, 1122 (2004).
8. Kononenko T.V., Meier M., Komlenok M.S., Pimenov S.M., Romano V., Pashinin V., Konov V.I. *Appl. Phys. A: Mater. Sci. Process.*, **90**, 645 (2008).
9. Claps R., Raghunathan V., Dimitropoulos D., Jalali B. *Opt. Express*, **12**, 2774 (2004).
10. Boyraz O., Jalali B. *Opt. Express*, **12**, 5269 (2004).
11. Sjodin T., Petek H., Dai H.L. *Phys. Rev. Lett.*, **81**, 5664 (1998).
12. Sabbah A.J., Riffe D.M. *Phys. Rev. B*, **66**, 165217 (2002).
13. Agranat M., Ashitkov S., Anisimov S., Ovchinnikov A., Shvartsburg A., Sitnikov D., Fortov V. *Appl. Phys. A: Mater. Sci. Process.*, **94**, 879 (2009).
14. Nejadmalayeri A.H., Herman P.R., Burghoff J., Will M., Nolte S., Tunnermann A. *Opt. Lett*., **30**, 964 (2005).
15. Tallents G.J. *J. Phys. D: Appl. Phys.*, **17**, 721 (1984).
16. Sarkisov G.S. *Kvantovaya Elektron*., **25**, 41 (1998) [*Quantum Electron*., **28**, 38 (1998)].
17. Dinu M., Quochi F., Garcia H. *Appl. Phys. Lett.*, **82**, 2954 (2003).
18. Lin Q., Zhang J., Piredda G., Boyd R.W., Fauchet P.M., Agrawal G.P. *Appl. Phys. Lett.*, **91**, 021111 (2007).
19. Kononenko V., Konov V., Dianov E. *Opt. Lett.*, **37**, 3369 (2012).
20. Quere F., Guizard S., Martin P., Petite G., Gobert O., Meynadier P., Perdrix M. *Appl. Phys. B: Lasers Opt.*, **68**, 459 (1999).
21. Temnov V.V., Sokolowski-Tinten K., Zhou P., El-Khamhawy A., von der Linde D. *Phys. Rev. Lett.*, **97**, 237403 (2006).